ORIGINAL PAPER

Glyphosate adsorption onto porous clay heterostructure (PCH): kinetic and thermodynamic studies

Sabrine Besghaier[1] · J. A. Cecilia[2] · Nesrine Chouikhi[1] · E. Vilarrasa-García[3] · E. Rodríguez-Castellón[2] ·
Mohamed Chlendi[1] · Mohamed Bagane[1]

Abstract
The synthesis of PCH from natural bentonite produces a porous heterostructure material effective for the adsorption of glyphosate from water. The adsorption process takes place through an interaction between the silanol group of montmorillonite and/or the PCH adsorbent with the functional groups of glyphosate. The glyphosate adsorption isotherms, recorded for all the studied samples, have been established to be of Langmuir type. The kinetic of the herbicide adsorption on the PCH was best described by the pseudo-second-order model. With the increase in temperature from 25 to 50 °C, the sorption capacities of the materials studied towards glyphosate increased. The process of glyphosate adsorption was found to be endothermic and spontaneous in nature, as indicated by positive values of ΔH and negative values of ΔG. According to the results obtained, the herbicide sorption was more effective in a basic environment. The maximum amount of adsorbed glyphosate is almost doubled with PCH from 13.5 mg/g of natural clay to 27.5 mg/g of PCH.

Graphic abstract
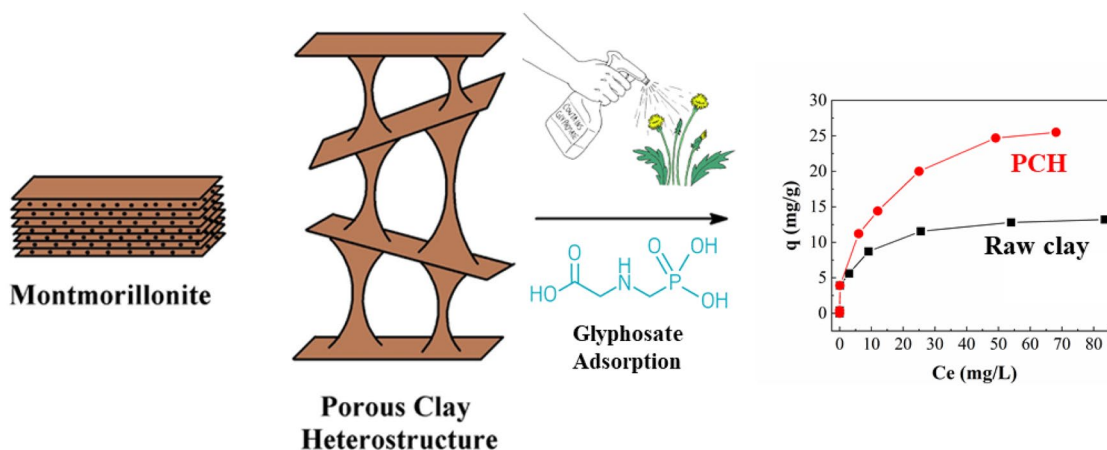
✉ J. A. Cecilia
jacecilia@uma.es

✉ E. Rodríguez-Castellón
castellon@uma.es

1   Research Laboratory of Applied Thermodynamic, National Engineering School of Gabes, University of Gabes, 6029 Gabes, Tunisia

2   Department of Inorganic Chemistry, Crystallography and Mineralogy, Universidad de Málaga, Campus de Teatinos, 29071 Malaga, Spain

3   Department of Chemical Engineering, Grupo de Pesquisa em Separações por Adsorção, Universidade Federal do Ceará, Campus do Pici, Fortaleza, CE 60455760, Brazil

Introduction

Research on sustainable wastewater treatment technologies has intensified in recent decades because of growing public concern about environmental issues and more severe regulations related to water pollution. Water pollution is caused by the discharge of dirty water from the domestic activities (washing and cleaning various, evacuation of domestic urine and excrements, etc.) and also by various industrial and agricultural activities which produce foods, chemicals compounds, dyes and energy. Pesticides are chemicals compounds that are used in industrial, forestry or farming sites to control of vegetation, insects and rodents (Aktar et al. 2009; Marican and Durán-Lara 2018).

According to their chemical composition, pesticides can be classified into organochlorines, organophosphorus, chlorophenols, carbamates or pyrethroids (Hamza et al. 2016; Marican and Durán-Lara 2018). These pesticides access the environment due to accidents or negligence such as percolation from storage and disposal sites in industrial facilities as well as spills in the transportation step (Khan et al. 2004). In the case of the pesticides used to control pests in crops, they seep into soils and enter surface watercourses and groundwater (Hamza et al. 2016). Nowadays, these pesticides have affected the water tables, which causes problem for human health because these compounds are very stable and can persist for a long time in soil and water (Odukkathil and Vasudevan 2013). Also, they can cause chronic damage and anomalies in both fauna and flora (Jariyal et al. 2015).

Focusing on organophosphate compounds, these chemicals are mainly used in pest control as an alternative to chlorinated hydrocarbons, which are more persistent in the environment. Although organophosphates are considered highly effective insecticides some of them, such as sarin and VX nerve agents are extremely toxic to humans (Hayes et al. 1980). In fact, organophosphates had an exclusively military application during the Second World War due to their neurotoxic effects, being subsequently used in the agricultural industry (Eto 1974). Thus, since 1950, organophosphate compounds such as parathion and malathion have been consolidated as agricultural insecticides (Eto 1974; Wilkinson and Wilkinson 1976). These pesticides are formed by a phosphorus atom linked to 4 oxygen atoms or 3 oxygen atoms and 1 sulfur in some cases. One of the phosphorous-oxygen bonds is weak and the atom of phosphorus released from this group is associated with acetylcholinesterase which is responsible for breaking down the medium of acetylcholine (it also plays an important role in the central nervous system). When the acetylcholine is destroyed, nervous hyperactivity occurs that can causes the death of animals (Eto 1974; Wilkinson and Wilkinson 1976).

Glyphosate ($C_3H_8NO_5P$) was introduced as a nonselective herbicide in the 1970s, and has become one of the most extensively used herbicides worldwide (Wang et al. 2016). Recently, glyphosate has been reported to be very harmful as it is involved in many maladies such as Alzheimer and Parkinson's disease, depression, cancer, infertility including genotoxic effects. The International Agency for Research on Cancer (IARC) has classified glyphosate as a 37 "probable human carcinogen" due to its mutagenic, genotoxic, and carcinogenic effects which explains the fact that the use of this herbicide is banned in 17 countries in the world as Belgium, France, Italy, USA, Oman Saudi Arabia Kuwait Emirates and United Arab (Sarkar and Das 2017).

There are many procedures for waste treatment such as photocatalytic degradation, combined photo-Fenton, biological oxidation, advanced oxidation processes, aerobic degradation, nano-filtration membranes and ozonation (Marican and Durán-Lara 2018). However, these methods are not the solution due to their high cost and low efficiency on a larger scale. Adsorption is one of the most important processes for the removal of pesticides due to its mechanical stability, low specificity, fast kinetics adsorption and high adsorption capacity (Halim et al. 2010). In this sense, it has been reported that porous carbons such as carbon nanotubes (Dehghani et al. 2017; Sarkar and Das 2017), biochar (Jiang et al. 2018), activated carbon prepared from Lawsonia inermis wood (Omri et al., 2016) or graphene-based composites (Suo et al. 2018; Yang et al. 2017), metal organic frameworks (MOFs) (Jamali et al. 2019; Yang et al. 2018a), mesoporous silica (Chen et al. 2020) or calcium alginate hydrogel fibers decorated with zirconium nanoparticle s (Zare et al. 2016). Most of these adsorbents are very effective on a laboratory scale. However, the synthesis of materials in industry can cause a reduction of the textural properties at such a high cost due to the complicated process.

That is why it is necessary to develop low-cost adsorbents to have a competitive and sustainable adsorption process. Therefore, clay minerals have emerged as a suitable choice due to their excellent performance in the areas of adsorption and catalysis for many industrial applications. In addition, the high availability, stability, abundance of unlimited applicability in the field of water and gas treatment gives them potential for use in pesticide removal processes (Adeyemo et al. 2017; Zhu et al. 2016).

Generally, the partial substitution of Si^{4+}-species by Al^{3+}-species generates a positive charge deficiency in the tetrahedral sheet, which is counterbalanced with the incorporation of alkaline cations in the interlayer spacing. Therefore, these phyllosilicates display a good cationic exchange capacity and layer expansion capacity (Brigatti et al. 2013). This proves that adsorption of pesticides is feasible on clay minerals because it is an inexpensive and environmentally friendly adsorbent. These materials can

be modified by intercalation of cationic compounds, heat treatment and acid activation to improve their textural properties (Cecilia et al. 2018b; Vaccari 1999).

The porous clay heterostructure (PCH) was first described by Galarneau et al. (1995) using similar templates as previously reported for mesoporous silicas as MCM-family (Beck et al. 1992). The synthesis of PCHs begins with an exchange of an alkaline cation, which is located in the interlayer space for a bulky cation (cationic surfactant), subsequently, a source of silicon is added as an alkoxide and it expands around the cationic surfactant. Finally, a porous material is produced after calcination to remove organic matter. This material, PCH, plays the role of an excellent adsorbent or catalytic support since it combines micro and mesoporosity in its framework (Cecilia et al. 2015, 2018a, c). In the adsorption field, PCHs have been used for the adsorption of molecules with variable dimensions. Thus, these materials have been used in the CO_2 adsorption (Vilarrasa-García et al. 2017), the selective separation of small hydrocarbons (Pires et al. 2004, 2008), volatile organic compounds (Ferreira et al. 2006; Nunes et al. 2008), drugs (Gârea et al. 2015) and dyes (Aguiar et al. 2017).

The aim of this work is the synthesis of PCHs from natural Tunisian clay for the adsorption of glyphosate. The prepared materials were characterized by XRD, FTIR, TGA, XPS and BET measurements.

Materials and methods

Reagents

All of the reagents used in the present study were of analytical grade and used without further purification: sulfuric acid (95–98%, Aldrich), hexadecyltrimethylammonium bromide (99%, Aldrich), anhydrous n-propanol (99.9%, VWR), hexadecylamine (90%, Aldrich), tetraethylorthosilicate (98%, Aldrich), ethanol (96%, Aldrich). The glyphosate was supplied for LGC, Dr. Ehrenstorfer (Purity: 98.6%).

Clay minerals

The clay was collected from "Jebel Al Aidoudi in El Hamma-Gabes" (Tunisia). For purification, the clay was suspended in deionized water for 24 h to obtain the clay fraction (< 2 μm). After washing, a wet sieving was performed to remove sterile and crystalline phases. In the next step, the clay was then dried at 105 °C in the oven for 24 h. Finally, the dried clay is crushed and sieved at 40 μm.

Synthesis of the PCHs

The synthesis of PCHs was carried out according the procedure proposed by Cecilia et al. elsewhere (Cecilia et al. 2013).

To increase the interlayer space, 5 g of Na-montmorillonite were mixed with 18 g of hexadecyltrimethylammonium bromide (HDTM-Br) in 200 mL of n-propanol. After stirring for 72 h, the suspension has undergone a filtration and washing with deionized water until the pH was neutral to remove the non-intercalated $HDTM^+$. Then, the solid was re-suspended in 500 mL of water and stirred for 24 h. After this time, a solution of 1.8 g of hexadecylamine (used as co-surfactant) and 50 mL of *n*-propanol were added to the mother solution and stirred for 24 h. In the next step, 25 mL tetraethylorthosilicate (TEOS) were dissolved in 25 ml *n*-propanol and added to the mother solution to form the silica-pillars around the co-surfactant in the interlayer spacing of montmorillonite. The obtained gel was stirred during 72 h and then was filtered and washed with water–ethanol and dried at 60 °C in air for 12 h. Finally, the surfactant was removed by calcination at 550 °C with a heating rate of 1 °C min^{-1} during 6 h.

Characterization of the adsorbents

X-ray diffractograms were collected on an automated X'Pert Pro MPD (PANalytical BV) diffractometer equipped with a Ge (111) primary monochromator (strictly monochromatic Cu Kα1 radiation) and an X'Celerator detector with a step of 0.017° working at 45 kV and 40 mA. The powder profiles were recorded between 10° and 70° in 2θ with a total measurement time of 30 min. Low angle measurements were obtained with the same configuration maintaining divergence and anti-divergence aperture at 1/16° and with Soller of 0.02 rad.

Attenuated total reflectance (ATR) was performed using a Bruker's Vertex70 FT-IR spectrophotometer model. The spectral acquisition was carried out using a standard spectral resolution of 4 cm^{-1} and 64 accumulations in the range (4000–500 cm^{-1}).

The textural properties of the starting clay and the PCHs were determined by the N_2 adsorption–desorption at -196 ºC by an automatic ASAP 2420 system from Micromeritics. Before the measurements, samples were outgassed at 200 °C and 10^{-4} mbar overnight. The specific surface area was estimated from the Brunauer–Emmett–Teller (BET) equation considering a N_2 cross section of 16.2 Å^2 (Brunauer et al. 1938). The total pore volume was calculated from the adsorption isotherm at P/P$_0$ = 0.996. Micropore volume was determined was determined from the t-plot method from Lippens and De Boer calculations (Lippens and De Boer

1965). Pore size distribution was determined using the density functional theory (DFT) (Landers et al. 2013).

Differential thermal analysis (DTA) and thermogravimetry analysis (TGA) data were taken on a Mettler-Toledo (TGA/DSC 1) analyzer from RT instruments (New Castle, DE). The temperature was varied from RT to 1000 °C at a heating rate of 5 °C min⁻¹. Measurements were carried out on samples in open platinum crucibles under air flow.

The surface of the studied solids was studied by X-Ray Photoelectron Spectroscopy (XPS) with a Physical Electronic PHI 5700 spectrometer using non monochromatic Mg-Kα radiation (300 W, 15 kV, 1253.6 eV). The spectra of powdered samples were registered with a constant pass energy values at 29.35 eV, using a 720 μm diameter circular analysis area. The XPS spectra obtained were analyzed with PHI ACESS ESCA-V6.0F software and processed using *Multipak 8.2B* package. The binding energy values were referenced to C 1 *s* signal (284.8 eV). Shirley type background and Gauss-Lorentz curves were used to determinate the binding energy.

Adsorption experiments

All adsorption experiments were realized at 22 °C. Batch experiments were carried out to study the impact of pH, adsorbent mass, contact time as well as adsorption isotherms. After preparing a pesticide stock solution with a concentration of 100 mg/L, adsorption experiments were performed in a rotatory shaker. For this aim, 40 mg of PCH were added to 50 mL conical tubes containing 10 mL of glyphosate solution. At the end of each experiment, the supernatant was collected and centrifuged for 15 min.

The pH of each pesticide solution was adjusted using 0.1 mol/L of NaOH and 0.1 mol/L of HCl. The adsorption of glyphosate on PCH was carried out in pH range of 2 to 12, PCH dosage (10–50 mg), stirring rate (50–400 rpm), initial glyphosate concentration (20–100 mg/L) and contact time (10–120 min).

The concentration of pesticide in liquid phase (supernatant) was determined by liquid chromatography-mass spectrometry (HPLC). The analysis instrument is equipped with a Dionex Ultimate 3000 liquid chromatograph (Thermo Scientifics), an H-ESI II ionization source (electrospray) and a TSQ Quantum Access triple quadrupole mass spectrometer. During preparation before injection, 15 μL of each sample is taken and diluted to 5 ml with milli-Q water. The samples are filtered with a 25 μm nylon filter. In the quantitative determination, standard glyphosate (99.7%) and glyphosate 2–13C were used as internal standard (IS) (Sigma Aldrich). The standards were prepared in mili-Q water at a concentration of 1 mg mL⁻¹.

The liquid chromatograph operates with a hypercarb column (5 μm × 100 mm × 2.1 mm) (Thermo Scientifics).

The injection volume is 5 μL. Mobile phase A: 1% formic acid in acetonitrile. Mobile phase B: 1% formic acid in milli Q water. Mobile phase C: 95% methanol and 5% milli Q. water. The flow rate of the mobile phase is 300 μL/min with an A gradient from 0 to 80% at 0.5 min, remaining 2.5 min. Then a regeneration of the column is carried out for 3 min with 100% of phase C.

The mass spectrometer has a spraying voltage 4500 V, sheath gas 35, auxiliary gas 10, sweeping gas 0, T-shaped lens 80, capillary temperature 350ºC and auxiliary gas temperature 230 ºC.

Using a syringe pump, a glyphosate standard and the internal standard were injected into the mass spectrometer. The transitions from the father ion to the son ion have been optimized using the automatic optimization function of the TraceFinder software, $\lambda_{glyphosate} = 220$ nm.

The amount of glyphosate adsorbed (adsorption capacity q) was calculated by using the following mass balance:

$$q = \frac{(C_0 - C_e) \times V}{m} \tag{1}$$

C_0 is the initial liquid concentration of glyphosate (mg mL⁻¹), C_e is the equilibrium liquid concentration of glyphosate (mg mL⁻¹), V is the volume solution (mL) and m is the mass adsorbent (g).

Modeling of adsorption isotherms

The Langmuir model describes the equilibrium distribution of the adsorbed ions between the solid and liquid phases. This isotherm is valid for monolayer adsorption on a surface containing a precise number of similar sites. The linear form of Langmuir equation is defined by the equation below (Al-Ghouti and Da'ana 2020):

$$\frac{C_e}{q_e} = \frac{1}{Q_0 b} + \frac{1}{Q_0} C_e \tag{2}$$

where q_e (mg/g) is the amount of adsorbed glyphosate per unit mass of adsorbent and C_e is the glyphosate concentration at the equilibrium. Q_0 is the maximum amount of the glyphosate per unit mass of adsorbent to form a complete monolayer on the surface bound at high C_e and b is a constant related to the affinity of the binding sites (L/mg).

The essential characteristics of the Langmuir model can be described by an additional constant called the separation factor R_L (also called the equilibrium parameter) (Al-Ghouti and Da'ana 2020). This factor is defined by the following equation:

$$R_L = \frac{1}{1 + bC_0} \tag{3}$$

where C_0 is the highest initial concentration of Glyphosate.

If $R_L = 0$, the adsorption is irreversible.

If $0 < R_L < 1$, the adsorption is favorable.

If $R_L = 1$, the adsorption is linear.

If $R_L > 1$, the adsorption is unfavorable.

The Freundlich model represents the adsorption on a heterogeneous surface and it is described with the following linear form (Al-Ghouti and Da'ana 2020):

$$\ln q_e = \ln K_F + \left(\frac{1}{n}\right) \ln C_e \tag{4}$$

where K_f (L/mg) and n are Freundlich constants with K_F is the adsorption capacity of the sorbent and n giving an indication of the adsorption process favorability (Al-Ghouti and Da'ana 2020).

The Temkin model is known with the linear form, which is presented by the equation below:

$$q_e = B \ln A + B \ln C_e \tag{5}$$

This model has an isotherm constant A (L/g) and a sorption heat constant b (J/mol) where $B = RT/b$; R is the gas constant (8.314 J/mol K) and T (K) is the absolute temperature.

Adsorption kinetics

Lagergren proposed a method for adsorption analysis, which is the pseudo-first-order kinetic equation in the linear form (Vaccari 1999).

$$\log\left(q_e - q_t\right) = \log q_e - \left(\frac{k_1}{2.303}\right)t \tag{6}$$

where q_e and q_t are the amount of glyphosate adsorbed (mg/g) at the equilibrium and at an instant t (min) and k1 is the pseudo-first-order rate constant (1/min).

A linear plot of $\ln(q_e-q_t)$ against time allows was found with a good correlation coefficient. The Lagergren's first-order rate constant (k_1) and q_e determined from the model are presented in Table 4 together with the corresponding correlation coefficients.

The pseudo-second-order kinetic model was proposed by Blanchard with and presented with the following equation in the linear form (Galarneau et al. 1995):

$$\frac{t}{q_t} = \frac{1}{k_2 q_e^2} + \frac{1}{q_e}t \tag{7}$$

where k_2 (g/mg h) is the rate constant of adsorption, q_e (mg/g) is the amount of glyphosate adsorbed at equilibrium and q_t (mg/g) is the amount of glyphosate adsorbed at time t. The equilibrium adsorption capacity (q_e), and the second-order constants k_2 (g/mg min) can be determined experimentally from the slope and intercept of plot t/q_t versus t.

Results and discussion

Characterization

The structure of the clay and PCH was analyzed by XRD and illustrated in Fig. 1. For the raw clay, d_{001} diffraction peak can be observed at $2\theta = 7.7°$ (11.7 nm). This indicates that the cations located in the interlayer spacing are partially solvated since the interlaminar spacing usually oscillates between 10 nm for the anhydrous clay and 14 nm in the case of clay with fully solvated cations (Cecilia et al. 2018a). Other diffraction lines that have been considered in the literature for smectites are located at $2\theta = 19.9°$, $34.9°$ and $62.1°$ (Cecilia et al. 2013). Among them, the latter diffraction peak is very useful since it is possible to discern between a dioctahedral and trioctahedral smectites. In the case of the clay of this research, the d_{060} reflection appears at $2\theta = 62.1°$ (1.49 nm). This indicates the presence of a dioctahedral clay, i.e. Al-rich smectite since the trioctahedral clay (Mg-rich smectite) should appear at 1.52 nm. In addition, the presence of narrower peaks also suggests the existence of impurities in the Al-rich smectite. Thus, it is noteworthy the presence of a peak located at $2\theta = 26.6°$, which is assigned of the existence of quartz. The presence of the other peaks is assigned of other impurities such as calcite or plagioclases.

The inclusion of a bulky cation and the formation of silica pillars should modify the basal diffraction peaks. However,
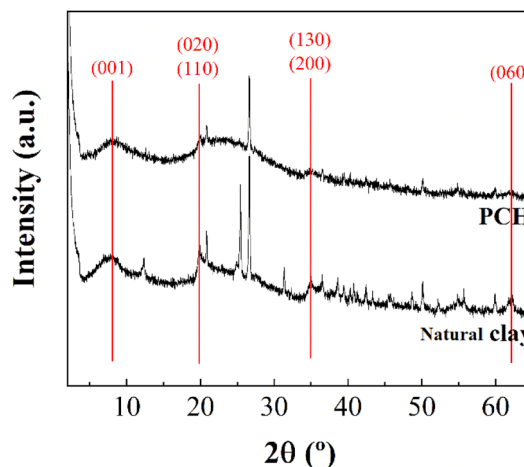

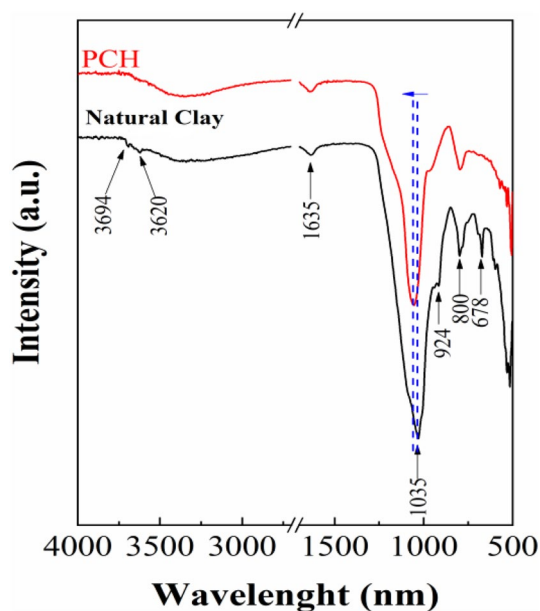**Fig. 1** XRD pattern of the Natural Clay raw clay and PCH

Fig. 2 FTIR-ATR spectra of Natural Clay and PCH

Fig. 3 N_2 adsorption–desorption isotherms at −196 °C for Natural Clay and PCH

basal reflections such d_{001} hardly change. Nevertheless, it is striking that the diffraction peaks are less intense after the insertion of the pillars, probably due to a partial delamination of the smectite, which causes a random displacement along the *a* and *b*-axes leading to a *house of cards* structure (Vilarrasa-García et al. 2017). On the other hand, it can also be observed that the amount of crystalline impurities decreases drastically since only the presence of quartz is observed.

Figure 2 illustrates the ATR spectra of the natural clay and the PCH. In the case of the raw clay, the OH-stretching region shows a broad band located between 3700 and 2700 cm^{-1}. In this region, it is noteworthy the presence of two bands located at 3694 and 3620 cm^{-1}. The band located at 3646 cm^{-1} is assigned to the Al(OH)Al-stretching vibrations while the band at about 3694 cm^{-1} is attributed to the presence of pyrophyllite-like local structural fragments (Zviagina et al. 2004) or to a small amount of Mg in the octahedral sheet of montmorillonite (Franco et al 2016). The Si–O stretching vibration of raw clay displays a maximum about 1035 cm^{-1}, which is in agreement with other data described for montmorillonite previously (Madejová 2003; Zviagina et al. 2004). On the other hand, the Al_2OH bending bands of montmorillonite about 924 cm^{-1} arises from vibrations of inner and surface OH groups (Madejová 2003) while the band located at 800 cm^{-1} is assigned to the overlapping of AlMgOH bending bands, which reflects partial substitution of Al-species in the octahedral sites by Mg-species (Madejová, 2003), and the Fe_2OH bending bands (Madejová 2003). The band located about 678 cm^{-1} is attributed to Fe–O out-of-plane vibration (Madejová 2003). Finally, the
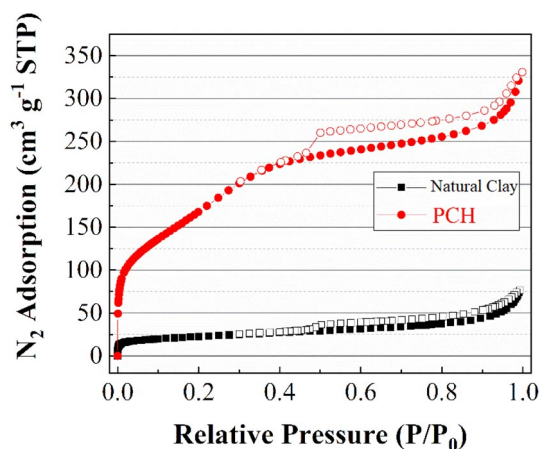
band located at 1635 cm^{-1} related to the water bending mode (Farmer 1974).

With regard to the PCH, the bands located between 3750–3525 cm^{-1}, assigned to the presence of silanol groups, disappear after the calcination of the organic matter. It must be considered that the combustion of organic matter is an exothermic process in such a way the –OH groups are probably condensed to siloxanes groups (Cecilia et al. 2013). On the other hand, it is also noteworthy that formation of silica pillars causes a slight shift of the Si–O stretching vibration as a consequence of the formation of amorphous silica (Madejová 2003).

To evaluate the textural properties of natural clay and PCH, N_2 adsorption/desorption isotherms at −196 °C on those adsorbents were carried out (Fig. 3). According to the IUPAC classification, both adsorbents can be considered as type IV, which is typical of mesoporous material, although the increase of the N_2 adsorbed at high relative pressure can resemble to type II, which is typical of macroporous materials (Thommes et al. 2015). In the same way, both adsorbents also display hysteresis loops that can be fitted to H_3, which are given by non-rigid aggregates of plate-like particles as clays (Thommes et al. 2015). The detailed analysis of the N_2-adsorption isotherms reveals that PCH adsorbs high amount of N_2 at lower relative pressure. This indicates that PCH displays higher micro-porosity than its corresponding natural clay. These data are in agreement with the literature since these materials have been used in adsorption processes for small molecules such as CO_2 or small hydrocarbons (Pires et al. 2008; Vilarrasa-García et al. 2017). At higher relative pressure, the increase of the N_2-adsorbed mainly for PCH suggests the presence of macro-porosity, which can be related to a disorder of the sheets during the formation of the PCH.

Table 1 Textural parameter of Natural Clay and PCH

Sample	S_{BET} (m^{2}g^{-1})	t-plot (m^{2}g^{-1})	Pore volume (cm^{3}g^{-1})	Micropore volume (cm^{3}g^{-1})
Natural Clay	69	38	0.082	0.018
PCH	621	422	0.441	0.227
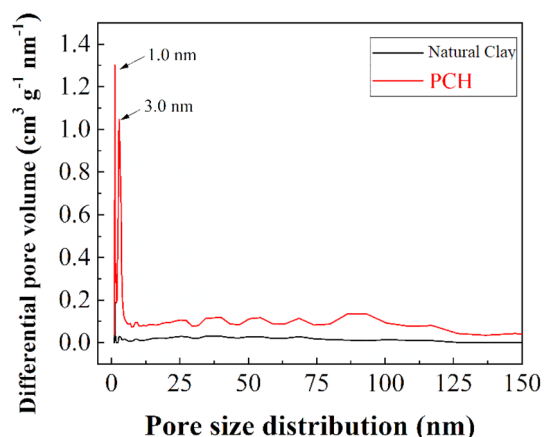
Fig. 4 Pore size distribution of PCH and Natural Clay sample

The specific surface area was determined from BET equation (Table 1) (Brunauer et al. 1938). These data show that PCH has much higher S_{BET} value than that shown by natural clay. In the same way, the PCH also displays a high microporosity in comparison to the natural clay as was inferred from its N$_2$-adsorption isotherm. With regard to the pore volume, the data reported in Table 1 follow the same trend to that observed for the specific surface area since PCH displays higher micro- and meso-porosity.

The pore size distribution was estimated by the DFT method and was reported in Fig. 4 (Landers et al. 2013). In the case of natural clay, a maximum located about 1 nm can be observed, which confirms the micro-porosity of the natural clay, being in agreement with XRD data where d$_{001}$ diffraction peak reported an interlayer spacing of 11.7 nm (Fig. 1). In the case of the pore size distribution of the PCH, two maxima located at 1.0 and 3.0 nm are observed so this material has a dual porosity. The greater intensity of the

band whose pore distribution is 1.0 nm confirms the presence of large micro-porosity as a consequence of a random shifting of the sheets in the clays along the synthesis of PCH. The signal whose pore distribution displays a maximum at 3.0 nm confirms the formation of a porous structure with homogeneous pore size in the PCH sample. From 3.0 nm, a wide pore size distribution can be observed due to voids between adjacent particles.

The surface chemical composition of the natural clay and PCH was determined by XPS (Table 2). In the case of the raw clay, the O 1 s core level spectrum shows a contribution betwenn 531.8–532.1 eV assigned to oxides species, The Al 2p core level spectrum shows a band at 74.9 eV while the Si 2p core level spectrum displays a band at 103.6 eV, which are typical for Al^{3+} and Si^{4+} of clay minerals, respectively. Other contributions with lower intensities are also observed in the case of the Mg 2p, Fe 2p and Ca 2p core level spectra, which are assigned to Mg^{2+}, Fe^{3+} and Ca^{2+} species. The analysis of the surface composition (in atomic concentration %) reveals a high proportion of Si in comparison to Al, Fe and Mg. Thus supposes that the substitution of Si by other cations with lower charge (Al, Fe and Mg) is relatively low so its cationic exchange capacity must also be relatively low. On the other hand, the presence of Fe an Mg-species also confirms the presence of AlMgOH and Fe$_2$OH bending bands shown in FT-IR section (Fig. 2).

The study of the PCH by XPS shows that the binding energy values of all the studied elements are maintained although, as expected, the atomic concentrations of these elements on the surface of the natural clay and the PCH differ between them. Thus, the analysis of the Si 2p core level spectrum of the PCH shows a clear increase of the Si-content on its surface, which confirms the presence of silica pillars in its structure as suggested from the textural properties previously (Figs. 3, 4).

The thermogravimetric analyses of the natural clay and the PCH are shown in Fig. 5. The TG analysis of the natural clay reveals two mass losses. The first loss mass between 30 and 250 ºC is related to the progressive desorption of water molecules adsorbed on the surface of the clay and those water that interacts with the cations located in the interlayer spacing. The second mass loss, located between 400 and 700 °C, corresponds to the dehydroxylation of structural –OH groups located between the tetrahedral sheets of 2:1

Table 2 Chemical surface composition (in atomic concentration %) of the Natural Clay and PCH before and after glyphosate adsorption

Sample	Atomic concentrations (%)						
	C 1s	O 1s	Al 2p	Si 2p	Ca 2p	Fe 2p	Mg 2p
Natural Clay	7.72	54.26	2.42	23.23	0.37	0.60	0.20
Natural Clay AA	9.62	60.55	3.27	25.79	0.11	0.54	0.19
PCH	6.89	52.75	0.45	29.78	–	0.10	0.03
PCH AA	8.28	62.22	1.62	27.69	–	0.15	0.05
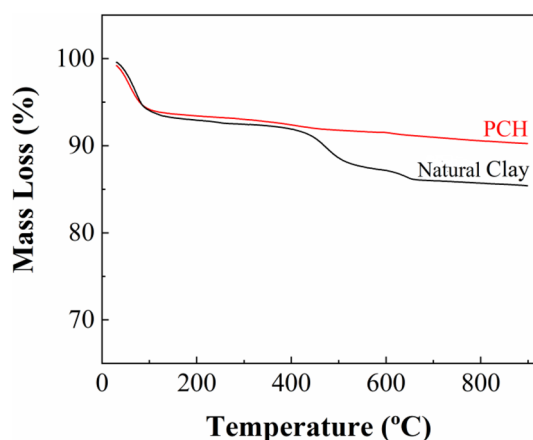
Fig. 5 Thermogravimetric analysis of the Natural Clay and PCH

Fig. 6 Effect of the pH on glyphosate adsorption onto PCH ($m_{PCH} = 40$ mg, T = 25 °C and $C_i = 100$ ppm)
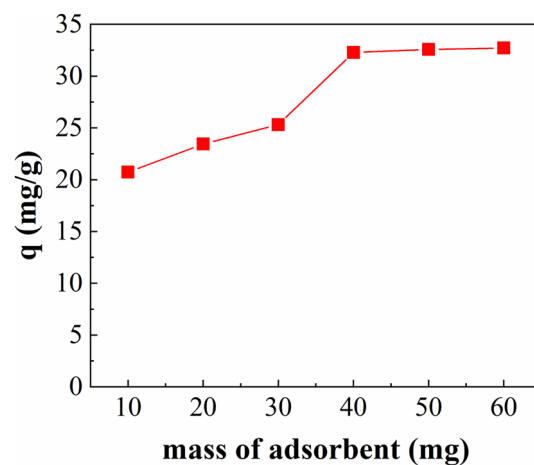
Fig. 7 Effect of the amount of PCH glyphosate adsorption (pH = 8, T = 25 °C and $C_i = 100$ ppm)

bentonite layers. Considering these two steps, the loss is 15%. In the case of the PCH, the first loss ascribed to the physisorbed water is very similar to that observed in the natural clay. However, the loss, ascribed to the dehydroxylation of –OH groups, is not observed in such a way the mass loss is only of 10%. This fact is ascribed to the calcination of the organic matter used as template in the synthesis of PCH, which is removed at 550 °C for 6 h (Garea et al. 2016).

Factors affecting the adsorption capacity

Once natural clay and PCH were characterized, both materials were used as sorbent in the adsorption of glyphosate, which is considered as a harmful herbicide.

Effect of the pH on glyphosate adsorption

pH is one of the most important parameters affecting the quality of groundwater. In addition, pH is a key parameter that profoundly influences the adsorption of the pollutant onto the adsorbent.

The study of the adsorption as a function of pH reveals that glyphosate adsorption grows from 19.09 to 32.57 mg/g when the pH of the solution increases from 2 to 12 (Fig. 6). These data show how the efficiency of the glyphosate adsorption improves in an alkaline medium. Under these pH conditions, the –O$^-$ groups of the natural clay or PCH can interacts with the –$^+$NH$_2$– groups of the glyphosate by electrostatic interaction (Khoury et al. 2010). These data are in agreement with those reported in previous investigations where the use of alkaline pH favors the glyphosate removal in forest soil or activated carbon (Herath et al. 2019; Sen et al. 2017).
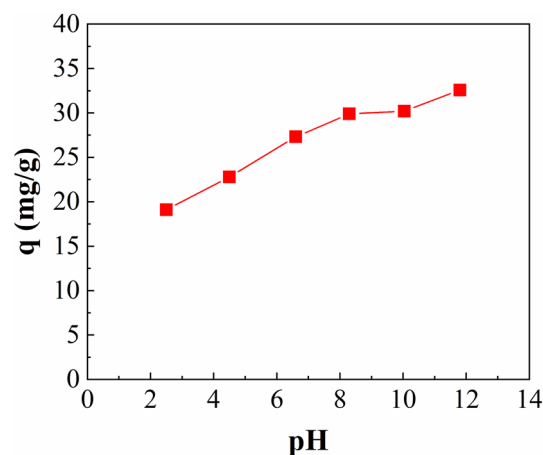
Effect of the amount of the PCH on glyphosate adsorption

In the present study, the initial pH of the glyphosate solution is 8 when initial glyphosate concentration, dosage and temperature were fixed at 100 mg/L, 5 g/L and 25.0 °C, respectively. The effect of changing the pH on the adsorption capacity of glyphosate is shown in Fig. 7.

The removal of glyphosate shows gradually increases as the amount of adsorbent in the dispersion increases from 0.01 to 0.04 g/10 mL. This is due to the increase in available adsorption sites (Fig. 7). It is also due to the enhancement of new surface area with the increase in the amount of the adsorbent. From this point, the glyphosate adsorption capacity with a mass of PCH greater than 0.04 g is almost constant and reaches the adsorption equilibrium.
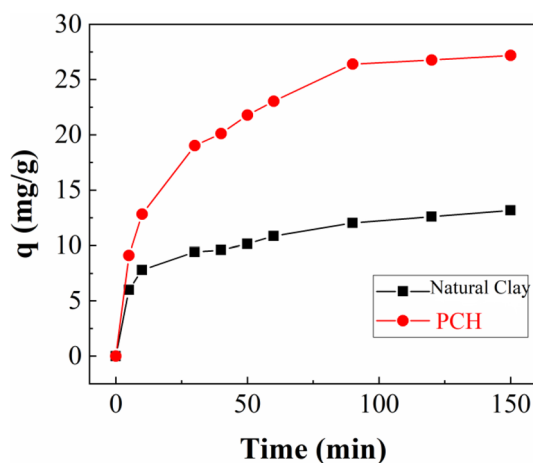
Fig. 8 Effect of contact time Glyphosate Adsorption onto Natural Clay (NC) and (PCH) using an initial Glyphosate concentration 100 ppm at pH = 8 and T = 25 °C
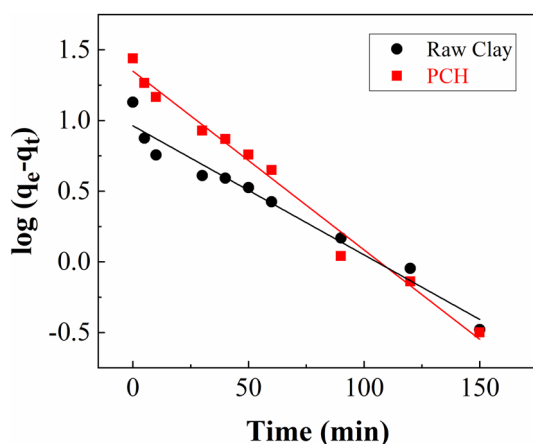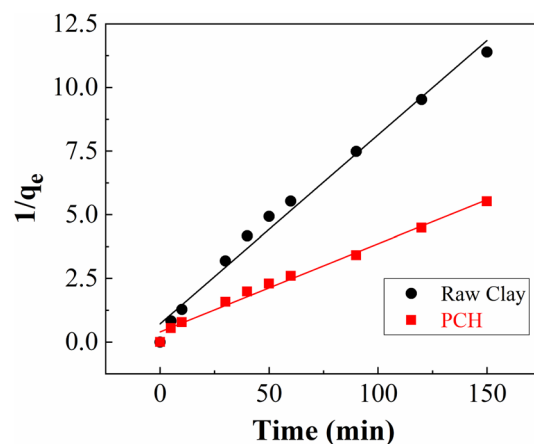

Fig. 10 Pseudo-second-order kinetic model of Glyphosate adsorption on Natural clay and PCH

It was observed that the pseudo second- order model better represented the adsorption kinetics and the calculated q_e values agreed with the experimental q_e values (Table 3). This suggests that the adsorption of glyphosate follows second order kinetics with both natural clay and PCH. The correlation coefficient value of the pseudo-first order kinetic equation is slightly lower than the pseudo-second order kinetic equation, indicating that this adsorption is mainly controlled by the surface control, rather than the adsorbate diffusion (Chen et al. 2016).

Equilibrium modeling

Figure 11 shows the adsorption isotherms of glyphosate on the starting clay and the PCH. The isotherms of both adsorbents are of type I. The isotherms have a marked initial slope that meaning at low concentration the materials are more efficient. The saturation of adsorbent is related to the occupation of adsorption sites. These data reveal that glyphosate adsorption on natural clay is about 13.2 mg/g while PCH displays higher adsorption values (25.5 mg/g) under similar conditions. The greater adsorption capacity of the PCH could be ascribed to a higher affinity due to its textural properties with a larger surface area and a high number of micropores. It is a consequence of the formation of SiO_2 pillar and the delamination of the clay sheets (Cecilia et al. 2013) in such a way this adsorbent can capture glyphosate molecules in its porous structure. The adsorption capacity of PCH is above other clay minerals although these values are below biochars and some soils (Table 4).

To carry out a more detailed study of the adsorption isotherms, both isotherms were fitted to Langmuir, Freundlich and Temkin models.

The plotting (C_e/q_e) versus (C_e), $(\ln q_e)$ versus $(\ln C_e)$ and (q_e) vs $(\ln C_e)$, it is possible to determine the constants of

Fig. 9 Pseudo-first-order kinetic model of Glyphosate adsorption on Natural clay and PCH

Adsorption kinetics

The kinetic profiles of glyphosate in raw clay and PCH are shown in Fig. 8. The kinetic study displays that both the natural clay and PCH require similar reaction time to reach the equilibrium conditions, about 100 min. This implies that the interaction between the adsorbate and the adsorbent must be similar in raw clay and PCH.

The modeling of glyphosate adsorption kinetics on natural clay and PCH was investigated using two common models, namely the pseudo-first order model and pseudo-second-order model (Figs. 9, 10). The second-order rate constant (k_2) and q_e determined from the model are presented in Table 3 along with the corresponding correlation coefficients.

Table 3 Kinetic adsorption parameters according to the pseudo first and second-order models for Glyphosate adsorption

Material	$q_{e,exp}$ (mg/g)	Pseudo-first-order kinetic model			Pseudo-second-order kinetic model		
		k_1 (min^{-1})	q_e (mg/g)	R^2	k_2 (min^{-1})	q_e (mg/g)	R^2
Natural clay	13.5	0.021	9.18	0.96	0.0076	13.5	0.99
PCH	27.5	0.029	22.37	0.97	0.0029	28.9	0.98

such model adsorption models. These constants are listed in Table 5.

The equilibrium data have been well described using the Langmuir model (Fig. 12) for the two materials with a correlation coefficient R^2 equal to 0.996 and 0.976 for the natural clay and the PCH respectively (Table 5). With Langmuir model, it assumes that glyphosate molecules are adsorbed on natural clay or PCH with monolayer adsorption in homogeneous adsorption sites. According to this model, the maximum adsorption capacity (Q_0) of the natural clay was 12.84 and 26.35 mg/g for the PCH, respectively. These data are close to the experimental values of maximum adsorption capacities. With regard to the b coefficient, which defines the interaction between adsorbate (glyphosate) and the adsorbent (natural clay or PCH), it can be observed that PCH displays a higher value in its parameter b (0.22 L mg^{-1}) in comparison to the raw clay (0.02 L mg^{-1}) (Table 5). This fact indicates that the interaction PCH-glyphosate-PCH is stronger with those observed in the case glyphosate-raw clay. Taking into account the textural properties and the characterization of the materials after the adsorption tests, it can be concluded that the interaction of the PCH with glyphosate in the microporous is stronger than the interaction natural clay with glyphosate, which is intercalated in the interlayer spacing as was deduced from XRD data (Fig. 2). The R_L values of natural clay and PCH are 0.3 and 0.04 respectively. This indicates that the adsorption of glyphosate on the natural clay and the PCH is favorable. From these data, it can be inferred that the PCH can be very useful for the removal of glyphosate from water.

The Freundlich model is very useful to determinate the heterogeneity of the adsorption sites (Fig. 13 and Table 6). K_f value, which defines the adsorption capacity of the sorbent, shows how PCH displays higher K_f values (5.26 L/mg) than natural clay one (2.38 L/mg). The values of the 1/n factor obtained from the Freundlich model are below unity in both cases (0.448 for natural clay and 0.409 for PCH). This fact indicates that, despite the adsorption isotherms were well-fitted to the Langmuir model; the adsorption sites are highly heterogeneous.

For the Temkin model (Fig. 14), the values of the heat of adsorption (b_T) are equals to 4.259 and 6.472 kJ/mol for raw clay and PCH, respectively. The value of the correlation factors (Table 7) confirms that the Temkin model is adequate for the adsorption of glyphosate by both adsorbents.

After adsorption studies, both natural clay and PCH were recovered and analyzed by several experimental techniques. From the study of the samples by XRD, it can be observed how the diffraction profile of the natural clay shows slight differences between before and after the adsorption process (Fig. 15). Thus, it can be observed how some peaks ascribed to impurities of the clay disappear after the glyphosate adsorption. However, the most striking fact is the displacement of the basal reflection (d_{001}) to lower 2θ values. This implies that glyphosate molecules tend to be introduced into the interlamellar spacing of smectite. On the other hand, no clear changes are observed in the diffraction profile of PCH after the adsorption process.

After adsorption process, it is expected that a slight change in the chemical composition on the surface could be observed both natural clay and PCH so XPS analysis were carried out (Table 2). These data show that the typical contributions of natural clay and PCH are maintained although it is noticeable a slight increase of the C-content on the surface of both samples, which could confirm the adsorption of glyphosate on their surface.

Temperature effect in the glyphosate adsorption on PCH

To understand the thermodynamic phenomenon of glyphosate adsorption on PCH, pesticide removal experiments
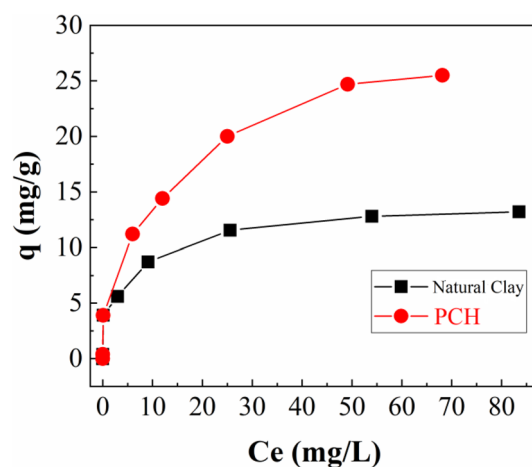

Fig. 11 Adsorption isotherms of Glyphosate onto Natural clay and PCH using an initial Glyphosate concentration (0.5–100 ppm) at pH = 8 and T = 25 °C

Table 4 Comparison between the glyphosate adsorption shown in the present work with that reported in the literature

Adsorbent	pH	Temperature (°C)	Qe (mg/g)	References
Goethite	7.0	25	7.9	Yang et al. (2018b)
Goethite	7.0	25	21.6	McConnell and Hossner (1985)
Magnetite	7.0	25	6.7	Yang et al. (2018b)
Ferrihydrate + NaCl	5.0	25	33	Pereira et al. (2019)
Hematite	7.0	25	7.9	McConnell and Hossner (1985)
Forest soil	12.0	30	161	Sen et al. (2017)
Soil	5.9	20	21	Gimsing et al. (2007)
Biochar	5.0	20	44	Mayakaduwa et al. (2016)
Biochar	2.0	30	35	Jiang et al. (2018)
Fe/carbon nanotubes	4.0	25	44	Diel et al. (2021)
$MnFe_2O_4$-graphene	4.7	25	39	Yamaguchi et al. (2016)
$MnFe_2O_4$@celullose activated carbon	3.4	25	167	Chen et al. (2019)
$MnFe_2O_4$ nanoparticles	3.4	25	93	Chen et al. (2019)
Montmorillonite	4.0	25	4.5	Glass (1987)
Illite	4.0	25	2	Glass (1987)
Kaolinite	4.0	25	1	Glass (1987)
Montmorillonite	4.0	25	5.2	da Cruz et al. (2007)
Kaolinite	4.0	25	6.5	da Cruz et al. (2007)
Bentonite	4.0	25	9.3	da Cruz et al. (2007)
Florai soil	4.0	25	0.4	da Cruz et al. (2007)
Tibagi soil	4.0	25	2.6	da Cruz et al. (2007)
Londrina soil	4.0	25	6.4	da Cruz et al. (2007)
Smectite	8.0	25	13	This work
PCH	8.0	25	26	This work

were performed varying the temperature of the contaminated solutions from 25 to 65 °C. From these data, it can be observed an increase of the glyphosate adsorption when the tempereture also increases Fig. 16. These data are in agreement with those reported in another study where glyphosate was adsorbed on an anionic exchange resin (Chen et al. 2016). Within the porous structure of the PCH the barrier of activation energy is overcome, which leads to the increase in the amount of the adsorbed pesticide.

The changes of enthalpy (ΔH°), entropy (ΔS°) and the Gibbs free energy (ΔG°) were determined using the following equations:

$$\Delta G = -RT \ln K_c \tag{8}$$

$$\ln K_c = \frac{\Delta S}{R} - \frac{\Delta H}{RT} \tag{9}$$

where R is the universal gas constant, T the absolute temperature and K_c is the adsorption constant (Garshasbi et al.

Table 5 Equilibrium adsorption parameters according to Langmuir model

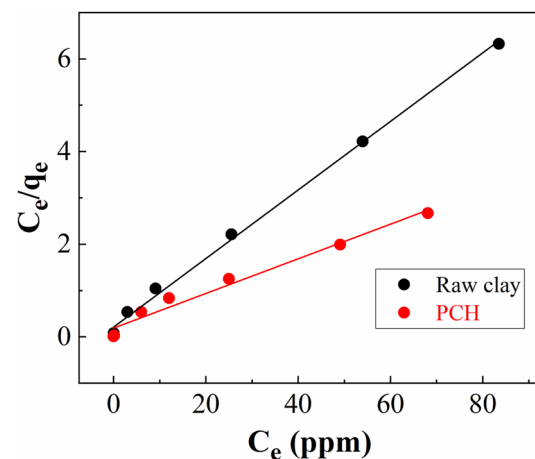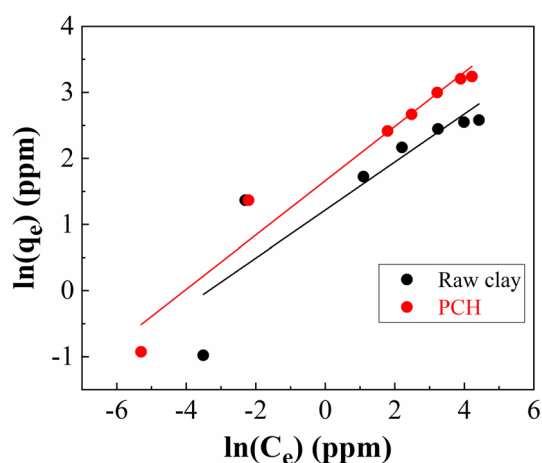| Adsorbent	Q_0(mg/g)	b(L/mg)	R^2	RMSE
Natural Clay	12.84	0.02	0.996	1.85 E-7
PCH	26.35	0.22	0.976	1.85 E-7

Fig. 12 Langmuir adsorption isotherm of glyphosate on Natural Clay and PCH

Table 6 Equilibrium adsorption parameters according to Freundlich model

Adsorbent	K_f (L/mg)	n	R^2	RMSE
Natural Clay	2.38	2.23	0.796	4.27 E-3
PCH	5.26	2.44	0.95	1.19 E-4

Table 7 Equilibrium adsorption parameters according to Temkin model

Adsorbent	A(L/g)	B	R^2	RMSE
Natural Clay	14.087	1.731	0.976	1.85 E-5
PCH	83.58	2.63	0.887	9.48 E-4

Fig. 14 Temkin adsorption isotherm of Glyphosate on Natural Clay (NC) and PCH

Fig. 13 Freundlich adsorption isotherm of glyphosate on Natural Clay and PCH

Fig. 15 XRD pattern of the Natural Clay and PCH before and after glyphosate adsorption

2017). The thermodynamic parameters were calculated by plotting $\ln K_c = f(1/T)$.

Table 8 presents the values of the thermodynamic parameters ($\Delta G°$, $\Delta H°$ and $\Delta S°$) for glyphosate adsorption on PCH. From these data, it can be inferred that the adsorption is an endothermic process ($\Delta H° > 0$). When $\Delta H°$ is in the range of 5–10 kJ mol^{-1}, the adsorption mechanism is physisorption; i.e., the bond between adsorbent and adsorbate is mainly due to van der Waals interactions. However, if $\Delta H°$ is in the range of 30–70 kJ mol^{-1}, the adsorption belongs to chemisorption; i.e., a chemical bond is formed between the adsorbate and the surface. In the present system, the value of $\Delta H°$ indicates that the adsorption is eminently physical so it is favored when the temperature increases (Li and Li 2009; Yan et al. 2008).

$\Delta S°$ is also positive so the degree of freedom increases at the solid–liquid interface during the adsorption process. The negative value of $\Delta G°$ of the PCH-glyphosate system

indicates that the reaction is spontaneous. It can be noted that the value of $\Delta G°$ decreases with increasing of the temperature, which can be explained by the fact that the adsorption becomes easier and favored when the temperature becomes very high so the degree of spontaneity of the thermodynamic reaction increases.

Conclusions

Bentonite is an effective precursor for synthesizing PCHs for glyphosate removal, concluding that these adsorbents can remove herbicides remaining in agricultural wastewater. The maximum amount of adsorbed glyphosate is almost doubled
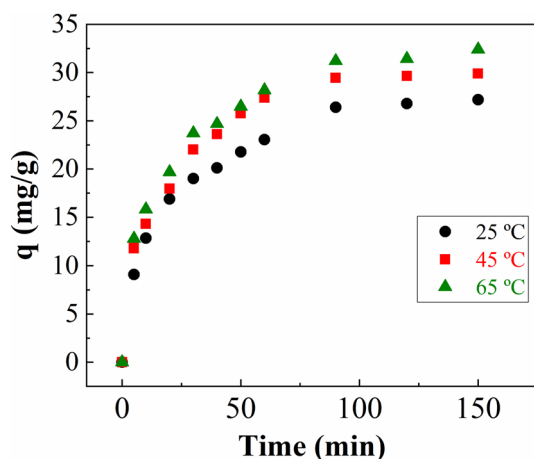
Fig. 16 Effect of the temperature on the removal of glyphosate onto Si-PCH (pH = 8, m = 40 mg and C_i = 100 ppm)

Table 8 Thermodynamic parameters for the Glyphosate adsorption onto Si-PCH

Temperature (°C)	$\Delta G°$(kJ/mol)	$\Delta H°$(kJ/mol)	$\Delta S°$(J/Kmol)
25	− 0.89	8.5	29.88
40	− 0.599		
50	− 0.105		

with PCH from 13.5 mg/g of natural clay to 27.5 mg/g of PCH.

The adsorption process takes place through an interaction between silanol groups of montmorillonite and/or of the PCH adsorbent with glyphosate. This adsorption is influenced by the pH of the system and the amount of adsorbent. The experimental results of the adsorption confirmed that PCH has a higher glyphosate adsorption capacity than natural clay.

Due to the vast existence of mineral clays and the simple processing for the synthesis of PCH, it is expected to have a significant impact on the fate of pesticides and other organic pollutants in the environment. Therefore, the mechanistic study of the adsorption of glyphosate on PCH may provide new insight into the fate of contaminants in the environment.

References

Adeyemo AA, Adeoye IO, Bello OS (2017) Adsorption of dyes using different types of clay: a review. Appl Water Sci 7:543–568

Aguiar J, Cecilia J, Tavares P, Azevedo D, Castellón ER, Lucena S, Junior IS (2017) Adsorption study of reactive dyes onto porous clay heterostructures. Appl Clay Sci 135:35–44

Aktar W, Sengupta D, Chowdhury A (2009) Impact of pesticides use in agriculture: their benefits and hazards. Interdiscip Toxicol 2:1–12

Al-Ghouti MA, Da'ana DA (2020) Guidelines for the use and interpretation of adsorption isotherm models: a review. J Hazard Mater 393:122383

Beck JS, Vartuli J, Roth WJ, Leonowicz M, Kresge C, Schmitt K, Chu C, Olson DH, Sheppard E, McCullen S (1992) A new family of mesoporous molecular sieves prepared with liquid crystal templates. J Am Chem Soc 114:10834–10843

Brigatti MF, Galan E, Theng B (2013) Structure and mineralogy of clay minerals. Dev Clay Sci 5:21–81

Brunauer S, Emmett PH, Teller E (1938) Adsorption of gases in multimolecular layers. J Am Chem Soc 60:309–319

Cecilia J, García-Sancho C, Franco F (2013) Montmorillonite based porous clay heterostructures: Influence of Zr in the structure and acidic properties. Microporous Mesoporous Mater 176:95–102

Cecilia J, Arango-Díaz A, Franco F, Jiménez-Jiménez J, Storaro L, Moretti E, Rodríguez-Castellón E (2015) CuO-CeO2 supported on montmorillonite-derived porous clay heterostructures (PCH) for preferential CO oxidation in H2-rich stream. Catal Today 253:126–136

Cecilia J, García-Sancho C, Vilarrasa-García E, Jiménez-Jiménez J, Rodriguez-Castellón E (2018a) Synthesis, characterization, uses and applications of porous clays heterostructures: a review. Chem Rec 18:1085–1104

Cecilia JA, Pardo L, Pozo M, Bellido E, Franco F (2018b) Microwave-assisted acid activation of clays composed of 2:1 clay minerals: a comparative study. Minerals 8:376

Cecilia JA, Soriano MD, Natoli A, Rodríguez-Castellón E, López Nieto JM (2018c) Selective oxidation of hydrogen sulfide to sulfur using vanadium oxide supported on porous clay heterostructures (PCHs) formed by pillars silica, silica-zirconia or silica-titania. Materials 11:1562

Chen FX, Zhou CR, Li GP, Peng FF (2016) Thermodynamics and kinetics of glyphosate adsorption on resin D301. Arab J Chem 9:S1665–S1669

Chen Q, Zheng J, Yang Q, Dang Z, Zhang L (2019) Insights into the glyphosate adsorption behavior and mechanism by a MnFe$_2$O$_4$@Cellulose-activated carbon magnetic hybrid. ACS Appl Mater Interfaces 11:15478–15488

Chen JL, Gao L, Jiang Q, Hou Q, Hong Y, Shen W-J, Wang Y, Zhu JH (2020) Fabricating efficient porous sorbents to

capture organophosphorus pesticide in solution. Microporous Mesoporous Mater 294:109911

da Cruz LH, de Santana H, Zaia CTBV, Zaia DAM (2007) Adsorption of glyphosate on clays and soils from Paraná State: effect of pH and competitive adsorption of phosphate. Braz Arch Biol Technol 50:385–394

Dehghani MH, Niasar ZS, Mehrnia MR, Shayeghi M, Al-Ghouti MA, Heibati B, McKay G, Yetilmezsoy K (2017) Optimizing the removal of organophosphorus pesticide malathion from water using multi-walled carbon nanotubes. Chem Eng J 310:22–32

Diel JC, Franco DSP, Nunes IS, Pereira HA, Moreira KS, Burgo TAL, Foletto EL, Dotto GL (2021) Carbon nanotubes impregnated with metallic nanoparticles and their application as an adsorbent for the glyphosate removal in an aqueous matrix. J Environ Chem Eng 9:105178

Eto M (1974) Organophosphorus pesticides: organic and biological chemistry. CRC Press, Cleveland, pp 254–255

Farmer VC (1974) Infrared spectra of minerals. Mineralogical Society, London

Ferreira P, Nunes C, Pires J, Carvalho AP, Brandao P, Rocha J (2006) Hydrophobic porous benzene-silica hybrid clay heterostructure and its application in the adsorption of volatile organic compounds. Mater Sci Forum 514:470–474

Franco F, Pozo M, Cecilia JA, Benítez-Guerrero M, Lorente M (2016) Effectiveness of microwave assisted acid treatment on dioctahedral and trioctahedral smectites. The influence of octahedral composition. Appl Clay Sci 120:70–80

Galarneau A, Barodawalla A, Pinnavaia TJ (1995) Porous clay heterostructures formed by gallery-templated synthesis. Nature 374:529–531

Gârea S, Mihai A, Ghebaur A, Nistor C, Sârbu A (2015) Porous clay heterostructures: a new inorganic host for 5-fluorouracil encapsulation. Int J Pharm 491:299–309

Garea S, Mihai A, Vasile E, Nistor C, Sarbu A, Mitran R (2016) Synthesis of new porous clay heterostructures: the influence of co-surfactant type. Mater Chem Phys 179:17–26

Garshasbi V, Jahangiri M, Anbia M (2017) Equilibrium CO_2 adsorption on zeolite 13X prepared from natural clays. Appl Surf Sci 393:225–233

Gimsing AL, Szilas C, Borggaard OK (2007) Sorption of glyphosate and phosphate by variable-charge tropical soils from Tanzania. Geoderma 138:127–132

Glass RL (1987) Adsorption of glyphosate by soils and clay minerals. J Agric Food Chem 35:497–500

Halim AA, Aziz HA, Johari MAM, Ariffin KS (2010) Comparison study of ammonia and COD adsorption on zeolite, activated carbon and composite materials in landfill leachate treatment. Desalination 262:31–35

Hamza RA, Iorhemen OT, Tay JH (2016) Occurrence, impacts and removal of emerging substances of concern from wastewater. Environ Technol Innov 5:161–175

Hayes AL, Wise R, Weir F (1980) Assessment of occupational exposure to organophosphates in pest control operators. Am Ind Hyg Assoc J 41:568–575

Herath GAD, Poh LS, Ng WJ (2019) Statistical optimization of glyphosate adsorption by biochar and activated carbon with response surface methodology. Chemosphere 227:533–540

Jamali A, Shemirani F, Morsali A (2019) A comparative study of adsorption and removal of organophosphorus insecticides from aqueous solution by Zr-based MOFs. J Ind Eng Chem 80:83–92

Jariyal M, Gupta V, Jindal V, Mandal K (2015) Isolation and evaluation of potent Pseudomonas species for bioremediation of phorate in amended soil. Ecotoxicol Environ Saf 122:24–30

Jiang X, Ouyang Z, Zhang Z, Yang C, Li X, Dang Z, Wu P (2018) Mechanism of glyphosate removal by biochar supported

nano-zero-valent iron in aqueous solutions. Colloids Surf A 547:64–72

Khan FI, Husain T, Hejazi R (2004) An overview and analysis of site remediation technologies. J Environ Manag 71:95–122

Khoury GA, Gehris TC, Tribe L, Sánchez RMT, dos Santos Afonso M (2010) Glyphosate adsorption on montmorillonite: An experimental and theoretical study of surface complexes. Appl Clay Sci 50:167–175

Landers J, Gor GY, Neimark AV (2013) Density functional theory methods for characterization of porous materials. Colloids Surf A 437:3–32

Li QQ, Li WM (2009) Study on thermodymamics of adsorbing timosaponin by resin. J Liaoning Univ Tradit Chin Med 6:

Lippens BC, De Boer J (1965) Studies on pore systems in catalysts: V. The t method. J Catal 4:319–323

Madejová J (2003) FTIR techniques in clay mineral studies. Vib Spectrosc 31:1–10

Marican A, Durán-Lara EF (2018) A review on pesticide removal through different processes. Environ Sci Pollut Res 25:2051–2064

Mayakaduwa SS, Kumarathilaka P, Herath I, Ahmad M, Al-Wabel M, Ok YS, Usman A, Abduljabbar A, Vithanage M (2016) Equilibrium and kinetic mechanisms of woody biochar on aqueous glyphosate removal. Chemosphere 144:2516–2521

McConnell JS, Hossner LR (1985) pH-dependent adsorption isotherms of glyphosate. J Agric Food Chem 33:1075–1078

Nunes CD, Pires J, Carvalho AP, Calhorda MJ, Ferreira P (2008) Synthesis and characterisation of organo-silica hydrophobic clay heterostructures for volatile organic compounds removal. Microporous Mesoporous Mater 111:612–619

Odukkathil G, Vasudevan N (2013) Toxicity and bioremediation of pesticides in agricultural soil. Rev Environ Sci Biotechnol 12:421–444

Omri A, Wali A, Benzina M (2016) Adsorption of bentazon on activated carbon prepared from Lawsonia inermis wood: Equilibrium, kinetic and thermodynamic studies. Arab J Chem 9:S1729–S1739

Pereira RC, Anizelli PR, di Mauro E, Valezi DF, da Costa ACS, Zaia CTBV, Zaia DAM (2019) The efect of pH and ionic strength on the adsorption of glyphosate onto ferrihydrite. Geochem Trans 20:3

Pires J, Araujo A, Carvalho A, Pinto M, Gonzalez-Calbet J, Ramırez-Castellanos J (2004) Porous materials from clays by the gallery template approach: synthesis, characterization and adsorption properties. Microporous Mesoporous Mater 73:175–180

Pires J, Bestilleiro M, Pinto M, Gil A (2008) Selective adsorption of carbon dioxide, methane and ethane by porous clays heterostructures. Sep Purif Technol 61:161–167

Sarkar S, Das R (2017) PVP capped silver nanocubes assisted removal of glyphosate from water—a photoluminescence study. J Hazard Mater 339:54–62

Sen K, Mondal NK, Chattoraj S, Datta JK (2017) Statistical optimization study of adsorption parameters for the removal of glyphosate on forest soil using the response surface methodology. Environ Earth Sci 76:22

Suo F, Xie G, Zhang J, Li J, Li C, Liu X, Zhang Y, Ma Y, Ji M (2018) A carbonised sieve-like corn straw cellulose–graphene oxide composite for organophosphorus pesticide removal. RSC Adv 8:7735–7743

Thommes M, Kaneko K, Neimark AV, Olivier JP, Rodriguez-Reinoso F, Rouquerol J, Sing KS (2015) Physisorption of gases, with special reference to the evaluation of surface area and pore size distribution (IUPAC Technical Report). Pure Appl Chem 87:1051–1069

Vaccari A (1999) Clays and catalysis: a promising future. Appl Clay Sci 14:161–198

Vilarrasa-García E, Cecilia J, Azevedo D, Cavalcante C Jr, Rodríguez-Castellón E (2017) Evaluation of porous clay heterostructures

modified with amine species as adsorbent for the CO2 capture. Microporous Mesoporous Mater 249:25–33

Wang S, Seiwert B, Kästner M, Miltner A, Schäffer A, Reemtsma T, Yang Q, Nowak KM (2016) (Bio) degradation of glyphosate in water-sediment microcosms—a stable isotope co-labeling approach. Water Res 99:91–100

Wilkinson CF, Wilkinson CF (1976) Insecticide biochemistry and physiology. Springer, New York

Yamaguchi NU, Bergamasco R, Hamoudi S (2016) Magnetic $MnFe_2O_4$-graphene hybrid composite for efficient removal of glyphosate from wáter. Chem Eng J 295:391–402

Yan L, Min Y, Hong-bin W (2008) Study on thermodynamics of soil adsorbing glyphosate. J Anhui Agric Sci 23:*

Yang Q, Wang J, Zhang W, Liu F, Yue X, Liu Y, Yang M, Li Z, Wang J (2017) Interface engineering of metal organic framework on graphene oxide with enhanced adsorption capacity for organo-phosphorus pesticide. Chem Eng J 313:19–26

Yang Q, Wang J, Chen X, Yang W, Pei H, Hu N, Li Z, Suo Y, Li T, Wang J (2018a) The simultaneous detection and removal of

organophosphorus pesticides by a novel Zr-MOF based smart adsorbent. Journal of Materials Chemistry A 6:2184–2192

Yang Y, Deng Q, Yan W, Jing C, Zhang Y (2018b) Comparative study of glyphosate removal on goethite and magnetite: adsorption and photo-degradation. Chem Eng J 352:581–589

Zare M, Ramezani Z, Rahbar N (2016) Development of zirconia nano-particles-decorated calcium alginate hydrogel fibers for extraction of organophosphorous pesticides from water and juice samples: facile synthesis and application with elimination of matrix effects. J Chromatogr A 1473:28–37

Zhu R, Chen Q, Zhou Q, Xi Y, Zhu J, He H (2016) Adsorbents based on montmorillonite for contaminant removal from water: a review. Appl Clay Sci 123:239–258

Zviagina BB, McCarty DK, Środoń J, Drits VA (2004) Interpretation of infrared spectra of dioctahedral smectites in the region of OH-stretching vibrations. Clays Clay Miner 52:399–410

Springer   ABEQ Associação Brasileira de Engenharia Química